Analyst

Accepted Manuscript

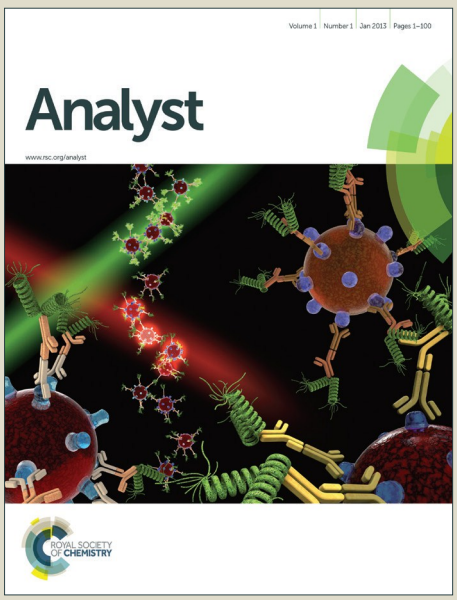

ROYAL SOCIETY OF CHEMISTRY

www.rsc.org/analyst

Journal Name

ARTICLE

Zeolitic imidazole framework templated synthesis of nanoporous carbon as a novel fiber coating for solid-phase microextraction†

Received 00th January 20xx,
Accepted 00th January 20xx

DOI: 10.1039/x0xx00000x

www.rsc.org/

Shuaihua Zhang, Qian Yang,‡ Zhi Li, Wenchang Wang, Chun Wang, Zhi Wang*

A new solid-phase microextraction (SPME) fiber coating material, a zeolitic imidazole framework-67 (ZIF-67) templated nanoporous carbon, Co-NPC, was fabricated by one-step direct carbonization of ZIF-67 without using any other carbon precursors. The prepared Co-NPC was then coated onto a functionalized stainless steel wire by a simple physical coating method to prepare SPME fiber. By coupling the Co-NPC coated fiber based SPME with gas chromatography/micro-electron capture detection (GC/μECD), the developed method exhibited low limits of detection (0.07- 0.45 ng g^{-1}) and wide linearity (0.30- 50 ng g^{-1}) for the determination of five organochlorine pesticides (OCPs) in vegetable samples. The method was applied to the analysis of cabbage, cucumber and celery cabbage samples, and the recoveries of the analytes were in the range of 87.9- 102.2% with the relative standard deviations (RSDs) ranging from 5.4% to 10.4% (n = 5). Single fiber repeatability and fiber-to-fiber reproducibility values expressed as RSDs were in the range of 4.9- 9.6% and 5.8- 11.0%, respectively. The method was simple, convenient and feasible for the determination of OCPs in real samples.

Introduction

As an efficient sample preparation technique, solid-phase microextraction (SPME)[1] can integrate sampling, extraction, and sample introduction into one step. SPME has been widely applied in sample preparations due to its being solvent-free, sensitive, simple, and also easy in automation and coupling with chromatographic techniques.[2, 3] The fiber coating material in SPME is critical for its extraction performance since SPME is based on the distribution equilibrium of the analytes between the sample matrices and the coating.[4, 5] Currently, many researchers focus on developing new SPME fibers and coatings with high extraction efficiency, long lifetime and low cost by using new preparation methods or new materials.[6] Till now, sol-gel,[7] chemical bonding,[8-10] electrochemical,[11] electrophoretic depositions,[12] and physical coating methods,[13, 14] have been successfully applied in the preparation of SPME fibers. For new coating materials, much research attention has been paid to the high-porosity materials, such as carbon nanotubes (CNTs),[15, 16] graphene,[8, 10] metal/metal oxide nanoparticles,[17, 18] and metal-organic frameworks (MOFs).[9, 19]

MOFs, also known as porous coordination polymers (PCPs), are a novel class of highly porous materials. In the last decade, they have received increased research interest due to their unique properties, such as high surface areas, tunable pore structures, high crystallinity and designable organic ligands.[20, 21] Zeolitic imidazolate frameworks (ZIFs) are a subclass of MOFs with zeolite or zeolite-like topologies, and they are composed of tetrahedral metal centers (Zn^{2+}, Co^{2+} and Cd^{2+}) connected by imidazole-based ligands. ZIFs possess several extraordinary features, such as chemical robustness and thermal stability.[22, 23] One of the most promising applications of MOFs in analytical chemistry seems to serve as novel coatings for SPME.[9] To date, quite a few MOFs, including MOF-199,[24] ZIF-8,[25] ZIF-7,[25] ZIF-90,[9] MAF-X8,[26] MIL-53,[27] MIL-101,[28] MIL-88B,[19] UiO-66,[29] IRMOF-3,[30] Cd(II)-MOF,[31] MOF-177,[32] Yb-MOF,[33] and bio-MOFs 100-102,[34] have been reported as fiber coatings for the SPME of benzene homologues,[24, 25] non-polar volatile organic compounds,[26, 28] n-alkanes,[25] polycyclic aromatic hydrocarbons,[27, 28, 30, 32, 33] endocrine disruptors,[9] polychlorinated biphenyls,[19, 32] and phenols[26, 29] in water samples. However, some MOFs showed a poor hydrothermal stability,[35] which hinders their further applications in SPME.

To solve the above problem, the exploration of MOFs as a precursor to construct nanoporous carbon (NPC) has recently become a burgeoning field.[36, 37] The main advantage of using a MOF as a template is that the MOF itself works as a precursor and contributes to the formation of high quality NPC.[38] Xu *et al.* have demonstrated the application of MOFs as a sacrificial template for the synthesis of NPC for the first time.[36] After that, several MOFs, such as MOF-5,[36, 37, 39] ZIF-8,[37, 39] Al-based PCP (Al-PCP),[39, 40] basolite Z1200 (BASF),[41] and isoreticular MOFs (IRMOFs, IRMOF-1, IRMOF-3, and IRMOF-8)[42] have been used as precursors to yield numerous NPCs with good properties in gas adsorption, electrochemical capacitance, sensing and catalysis. However, the report about the application of MOFs-templated NPC as a SPME coating is still very few.

*Department of Chemistry, College of Science, Agricultural University of Hebei, Baoding 071001, China. E-mail: wangzhi@hebau.edu.cn; zhiwang2013@aliyun.com; Fax: +86-312-7521513; Tel: +86-312-7521513

† Electronic supplementary information (ESI) available: The preparation of silver modified stainless steel wire, the effect of desorption time, and the comparison of sensitivity of different methods by various sorbents for the SPME of PAHs. See DOI: 10.1039/x0xx00000x

‡ Current address: Baoding municipal environmental protection bureau, Baoding 071000, China.

ZIF-67 ($Co(Hmim)_2$, Hmim = 2-methylimidazole) is formed by bridging 2-methylimidazolate anions and cobalt cations with a sodalite (SOD) topology.[43] The presence of Hmim ligands in ZIF-67 can eliminate the need for an additional carbon source, and it is possible to produce NPCs by direct carbonization.[44] In our current work, a MOF-templated NPC was fabricated by directly carbonizing the highly crystalline Co-based MOF without using any other carbon precursors.[45] The NPC was then coated onto a prior functionalized stainless steel wire by a simple physical coating method. The extraction characteristics of the ZIF-67 templated nanoporous carbon (Co-NPC) coated SPME fiber were investigated by using the fiber for the SPME of some organochlorine pesticides (OCPs). The important experimental parameters relevant to the extraction efficiency including extraction time, salt addition, stirring rate, desorption temperature and time were optimized. The analytical characteristics of the developed method with the use of direct-immersion SPME and gas chromatography/micro-electron capture detection (GC-μECD) were then evaluated under the obtained optimal conditions. The prepared fiber was applied to the extraction of OCPs from various vegetables including cabbage, cucumber and celery cabbage samples.

Experimental section

Reagents and materials

Cobalt nitrate hexahydrate ($Co(NO_3)_2{\cdot}6H_2O$) and Hmim were purchased from Aladdin-Reagent (Shanghai, China) and used without further purification. Methanol, ethanol and potassium chloride (KCl), all of analytical grade, were from Sinopharm Chemical Reagent (Shanghai, China). Neutral multifunctional silicone sealant was purchased from the local building materials market (Baoding, China). Double-distilled water was obtained from Yarong SZ-93A automatic double-distiller system (Shanghai, China). The stainless steel wires (type 304, 200 mm o. d.) used for the SPME fiber support were obtained from Shanghai Gaoge Industrial and Trading Co. (Shanghai, China).

The five OCP standards, i.e., 1,1-dichloro-2-(o-chlorophenyl)-2-(p-chlorophenyl) ethylene (*o,p′*-DDE), 1,1-dichloro-2,2-bis-(p′-chlorophenyl)ethylene (*p,p′*-DDE), 1,1-dichloro-2,2-bis-(p′-chlorophenyl)ethane (*p,p′*-DDD), 1,1,1-trichloro-2-(ochlorophenyl)-2-(p-chlorophenyl)ethane (*o,p′*-DDT) and 1,1,1-trichloro-2,2-bis(p′-chlorophenyl)ethane (*p,p′*-DDT), were obtained from AccuStandard Inc. (New Haven, USA). The OCP stock solutions were prepared in acetone at a concentration of 1.0 mg L^{-1} for each of the analytes and stored in the dark at 4 °C for further use. For method validation, the standard mixture solutions of different concentrations of the OCPs were prepared by a serial dilution of their corresponding stock solutions with double-distilled water.

Instrumentation

GC analyses were carried out on an Agilent 7820A series gas chromatograph (Agilent Technologies, CA, USA) equipped with a ^{63}Ni micro-electron capture detector (μECD) and a split/splitless injector. All the separations were performed on a HP-5 capillary column (30 m × 0.32 mm i.d. × 0.25 μm film thickness) (Agilent J&W Scientific, CA, USA). Nitrogen of high purity (> 99.999%) was used as both the carrier and the make-up gas at 1.2 mL min^{-1} and 25 mL min^{-1}, respectively. The GC chromatographic conditions for OCPs were as follows: splitless mode; injector temperature, 260 °C; detector temperature, 290 °C; the oven temperature program, starting at 60 °C for 2 min, then increased to 220 °C at 20 °C min^{-1}, finally increased to 260 °C at 5 °C min^{-1}, and held for 3 min.

The XRD patterns of the samples were measured on a Tongda TD-3500X X-ray diffractometer (Dandong, China) using Cu *Kα* radiation (40 kV, 150 mA) in the 2θ range from 10 to 60 °C. The size and morphology of the Co-NPC were observed by transmission electron microscopy (TEM) using a JEOL model JEM-2011(HR) (Tokyo, Japan) and scanning electron microscopy (SEM) on a Hitachi SU8020 field emission electron microscope (Tokyo, Japan). The specific surface area of the Co-NPC was measured by Brunauer-Emmett-Teller (BET) method using nitrogen adsorption and desorption isotherms on a Micromeritics 3Flex surface characterization analyser (Micromeritics instrument, USA). A thermogravimetric (TG) analyser (Henven HCT-2, Beijing, China) was applied to measure the thermal stability of the coating from room temperature to 700 °C under N_2 atmosphere at a heating rate of 10 °C min^{-1}.

Synthesis of Co-NPC

The Co-NPC was prepared *via* a two-step route, i.e., the fabrication of ZIF-67 and its subsequent calcination.[45, 46] The main scheme for the preparation of the Co-NPC is shown in Fig. 1. In the first step, the ZIF-67 nanoparticles were synthesized according to the reported method with some modifications.[47] Typically, 4 mmol of $Co(NO_3)_2{\cdot}6H_2O$ was first dissolved in 100 mL of methanol, while 16 mmol of Hmim was added to 100 mL of methanol in another glass vial. Then, the methanol solution of $Co(NO_3)_2$ was slowly added to the methanol solution of Hmim. The resulting mixture was stirred at ambient temperature for 6 h. Next, the precipitate was collected by centrifugation and washed repeatedly with ethanol. The obtained crystals were dried at 60 °C in a ventilation oven for 6 h and then in a vacuum oven at 100 °C for 12 h to obtain the product ZIF-67. In the second step, the as-prepared Co-MOF precursor was directly carbonized under a nitrogen flow at 700 °C for 6 h, starting from room temperature at a heating rate of 5 °C min^{-1}.[45] After the above calcination treatment, the purple precursor was converted into the black powder of Co-NPC.

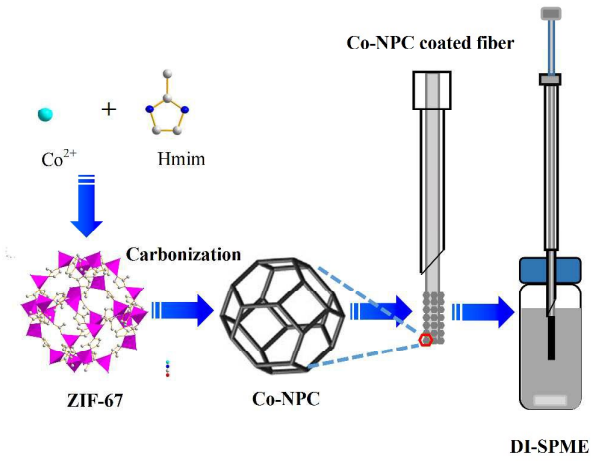

Fig. 1. Schematic illustration for the preparation of Co-NPC and its use for SPME.

Fabrication of Co-NPC coated SPME fiber

The stainless steel wires with a length of 20 cm were used to fabricate the Co-NPC coated SPME fibers. Before the coating, the stainless steel wire was first coated with microstructured silver layer by silver mirror reaction according to the reported methods.[8, 17] The functionalized stainless steel wire was dipped into silicone sealant[28] which had been diluted with toluene (w/v: 500 mg mL^{-1}) in a 1.5 mL Eppendorf tube, and then pulled out quickly. To get a uniform coating, the excessive glue on the stainless steel wire was wiped by a small piece of glass sheet. Next, the fiber was vertically inserted into the prepared Co-NPC powder in a 1.5 mL Eppendorf tube, rotated for a few cycles and then pulled out. Subsequently, the coated fiber was placed in an oven for conditioning at 150 °C for 30 min. The above process was repeated for several times until the desired thickness was obtained. At last, the coated wire was dipped into the diluted glue again to form a thin film of polymer which could protect the whole coating and avoid the flaking of the powder.[28] The coating thickness obtained after four coating cycles was around 60 µm, and the effect of Co-NPC coating thickness on the extraction performances is given in Fig. S1, ESI†. Prior to its use for SPME, the coated fiber was assembled to a 5 µL microsyringe and aged in the GC injector at 260 °C until a stable GC baseline was obtained.

Sample preparation and SPME procedures

Fresh samples (cabbage, cucumber and celery cabbage) were cut into small pieces and an aliquot of 100.0 g was homogenized using a food homogenizer. One gram of the homogenized sample was weighed and placed in a 10.0 mL centrifuge tube (for optimization experiments, 1.0 g of the homogenized sample was weighed and spiked with 5 µL of an appropriate concentration of the pesticide standard solution in a 10.0 mL centrifuge tube to get a spiked sample with a desired concentration). Then, 1.0 mL acetonitrile were added and mixed ultrasonically for 10 min. After centrifuged at 10 000 rpm for 5 min, the supernatant was transferred to a 15 mL glass vial and diluted to 10.0 mL using double-distilled water. Then, the vial was capped with a PTFE silicone septa. The outside needle of the fiber was used to penetrate the septa of the vial and then the coated fiber was directly immersed into the sample solution for SPME extraction at room temperature (see Fig. 1). After the extraction under a stirring at 600 rpm for 30 min, the fiber was withdrawn and immediately injected into the GC injector for thermal desorption at 260 °C for GC analysis. To eliminate the fiber carry-overs, the fiber was held in the injector for the whole run (21 min) before the next extraction.

Results and discussion

Characterization of the OMC-ZSM-5 coated fiber

The crystal structures of ZIF-67 and Co-NPC, were examined by wide-angle X-ray diffraction (XRD) measurements (Fig. 2). The relative intensity and peak positions in the XRD patterns of the ZIF-67 (Fig. 2A) matched well with the simulated patterns published in the literature (Fig. 2B),[46] confirming the successful synthesis of ZIF-67. The diffraction peaks observed in Co-NPC at around 2θ = 25° belong to a typical (002) interlayer peak of graphite-type carbon sheets (Fig. 2C). And the weak diffraction peaks derived from crystalline Co were also observed at 2θ = 45° and 52° in Fig. 2C.

The more structural and morphology information of the Co-NPC was further investigated by TEM and SEM. Due to the presence of Co in the Co-NPC, the obtained nanoporous carbons are constituted by both Co nanoparticles and carbon matrix.[48] As can be seen in Figs. 3A and 3B of the TEM images, the Co nanoparticles were incorporated in the carbon matrix. The SEM image shown in Fig. 3C gave a further evidence of the highly porous structure of the Co-NPC. Furthermore, the morphologies of the Co-NPC coated fiber on surface and cross-section were also investigated by SEM. As shown in Figs. 3D and 3E, the homogeneous and porous Co-NPC coating was obtained with the thickness of about 60 µm. Such porous structure increased the available surface area of the fiber coating, which was beneficial for the extraction performance.

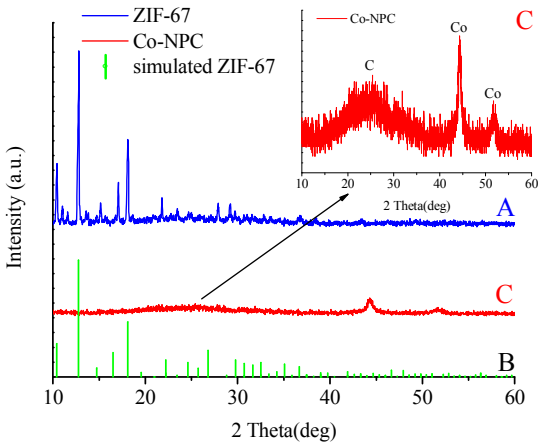

Fig. 2. XRD patterns of the synthesized ZIF-67 (A), simulated ZIF-67 (B) and Co-NPC (C).

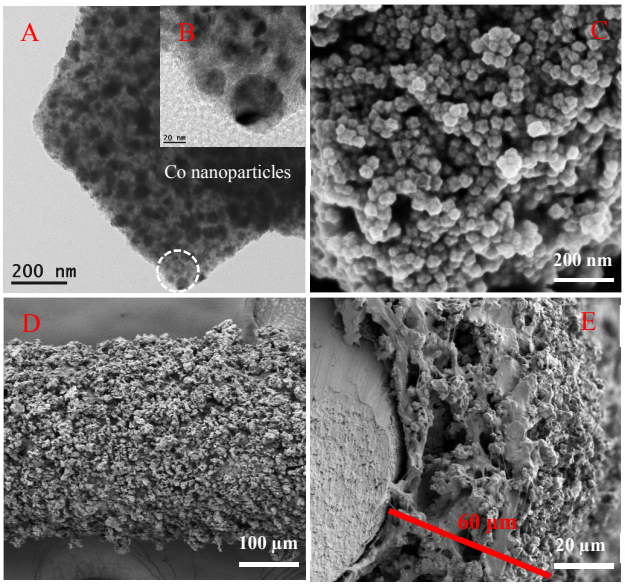

Fig. 3. Transmission electron micrographs of the Co-NPC with different magnifications (A) and (B); scanning electron micrograph of the Co-NPC (100 000×) (C) and the scanning electron micrographs of the Co-NPC coated fiber for (D) surface, 200× and (E) cross-section, 1000×.

To evaluate the specific surface area and the porosity of the Co-NPC, the N_2 adsorption-desorption isotherms and pore size distribution analysis were performed (Fig. 4). The general shape of the N_2 sorption isotherms for the Co-NPC (Fig. 4A) suggested the existence of different pore sizes spanning from micro- to meso-pores. The isotherms showed a drastic uptake at very low relative pressures, indicating the presence of micropores. And the following small slope observed at medium relative pressures as well as the desorption hysteresis denotes the existence of the mesopores. The BET specific surface area and total pore volume of the Co-NPC were calculated to be 342.6 $m^2 g^{-1}$ and 0.25 $cm^3 g^{-1}$, respectively, which are very close to the values from the previous report.[48] This means that the Co-NPC had a remarkable porous structure. Additionally, as shown in Fig. 4B, the pore sizes calculated by the Saito-Foley (SF) method were distributed from 0.51 to 1.18 nm.

The TGA measurements were made to evaluate the thermal stability of the Co-NPC fiber coating (Fig. S2, ESI†). The results showed that with the use of silicone as binder, the Co-NPC coated fiber was quite stable below 400 °C (98.4% of its weight remained at about 400 °C), and the fiber can endure the high temperatures for GC analysis.

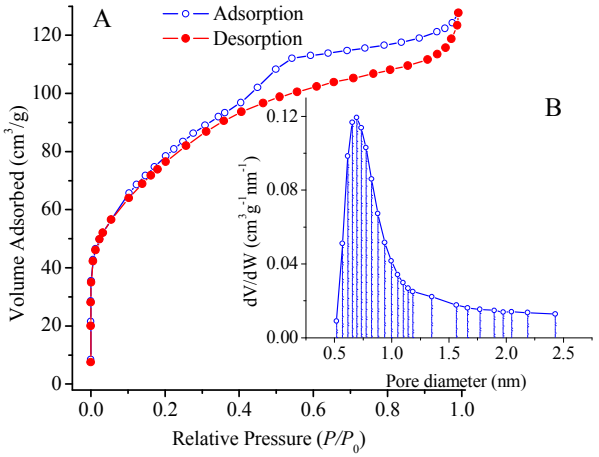

Fig. 4. (A) The N_2 adsorption-desorption isotherms and (B) Saito-Foley pore size distribution curve of the Co-NPC.

Optimization of SPME conditions

To achieve the best extraction efficiency of the Co-NPC coated fiber for the analytes, the main experimental factors that can affect the extraction, such as extraction time and temperature, salt addition, stirring rate, and desorption temperature and time, were investigated.

SPME is an equilibrium-based technique and the extracted amount of an analyte will be influenced by the extraction time. Therefore, the selection of extraction time is one of the critical steps in SPME method development. In this study, the effect of extraction time was investigated by varying the SPME time from 5 to 60 min while the other experimental conditions were kept unchanged. The relationship between the extraction time and peak areas of the OCPs is given in Fig. 5A. The result showed that the peak areas of the five OCPs were increased with increased extraction time and the extraction equilibrium was not achieved even after 60 min. Although the maximum extraction efficiency for the analytes may be obtained in the equilibrium situation, the analysis time will be prolonged. According to the nonequilibrium theory of SPME,[49] SPME quantitative analysis can be realized in a nonequilibrium situation if the extraction conditions are held constant. Therefore, making a compromise between the extraction time and the extracted amount of the analytes, the extraction time was chosen at 30 min.

The mass transfer rate of OCPs from water to the Co-NPC coated fiber was affected by the extraction temperature. The effect of the extraction temperature in the range from 20 °C to 60 °C was investigated. As shown in Fig. 5B, a suitable extraction temperature was found to be in the range of 20 °C to 30 °C. The higher extraction temperature caused a slight decrease of peak areas. Thus, room temperature (about 25 °C) was chosen for the extraction.

Salt addition can affect the extraction efficiency in SPME as a result of "salting-out" effect. Generally, for many organic compounds, their aqueous solubilities are decreased by salt addition.[50] This leads to a higher sorbent/sample distribution constant and increased extraction. The influence of ionic strength was studied by the addition of different KCl amounts, ranging from 0 to 30% (w/v). The results depicted in Fig. 5C shows that the addition of salt caused an increase in the extraction efficiency when the concentration of KCl was increased until 15%, and then a decrease in extraction efficiency of the analytes was observed when the amount of salt exceeded 15%. A possible reason for this could be the enhancement of solution viscosity at higher salt concentrations, which can decrease the mass transfer rate. Moreover, large amount of KCl in the sample solution might occupy the surface of the coating and it could have a negative effect on the extraction.[50, 51] According to the results obtained in this work, 15% (w/ v) of KCl was selected for the experiments.

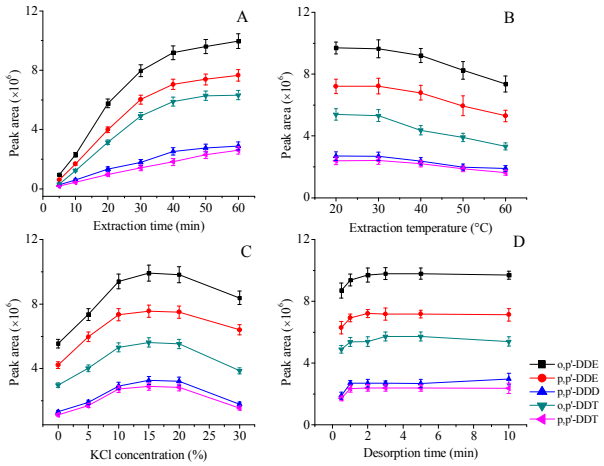

Fig. 5. Effect of (A) extraction time, (B) extraction temperature, (C) KCl concentration, and (D) desorption time. Conditions: analytes concentration, 100 ng L^{-1} each; stirring rate, 600 rpm; desorption temperature, 260 °C.

Generally, increasing the stirring rate can effectively accelerate the mass transfer of the analyte to the fiber coating and thus

enhance the extraction efficiency. The stirring rates ranging from 200 to 1000 rpm were tested to investigate this effect. The experimental results (Fig. S3, ESI†) showed that the agitation gave a positive effect on the exaction efficiency of the tested OCPs in the stirring rate range of 200- 600 rpm, and then a slight decrease in the extraction efficiency of the analytes was observed with further increase of the stirring rate. Thus, a stirring rate of 600 rpm was adopted for further experiments in view of higher extraction efficiency for the OCPs.

Optimization of the desorption conditions

In SPME, if the desorption time and temperature are not sufficient, the desorption process cannot be complete and the analytes will be remained on the sorbent.[50] As a result, the memory effect can be observed in next analyses. Therefore, both the time and temperature used for the desorption of the analytes from the fiber should be considered for optimization. In this study, the thermal desorption was investigated by varying the temperature of the injection port in the range of 200 - 290 °C. According to the results obtained, the peak areas of the analytes were enhanced with increased desorption temperature from 200 to 260 °C, and then remained unchanged with the further increase of the desorption temperature to 290 °C. In addition, the desorption time was evaluated in the range of 2-10 min and the experimental results (Fig. 5D) showed that the desorption between 2 and 10 min gave similar peak areas for the analytes. To eliminate the possible fiber carry-overs, the fiber was purged in the injector for the whole run before the next extraction. On the basis of the above results, the desorption at 260 °C for the whole time of the run was chosen for the experiments.

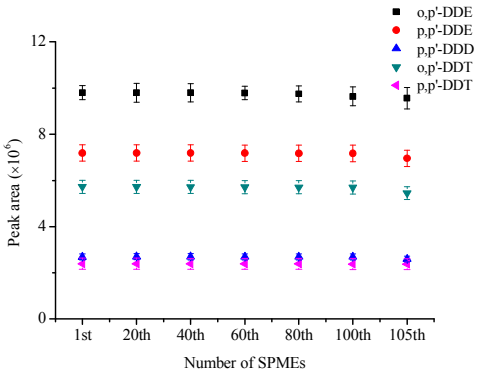

Fig. 6. Stability and lifetime of the Co-NPC coated fiber during the SPME extraction.

Possible extraction mechanism of the Co-NPC coating

To further understand the adsorption mechanism and selectivity of the Co-NPC coating for SPME, different types of organic compounds, including the five OCPs, 1,3,5-trichlorobenzene, 1,2,4-trichlorobenzene, 2,4-dichlorophenol, 2,4,6-trichlorophenol, 1-chlorohexane and 1-chlorooctane, were used as the model analytes for the study. The enrichment factor (EF) is defined as the ratio of the peak area of an analyte by SPME to the peak area by direct injection of 1 μL of the standard solution of the analytes at 1.0 μg L^{-1}, and log*P* is the octanol/water partition coefficient, which can serve as an indicator for the hydrophobicity of the analyte. A high EF value indicates a high extraction efficiency or high adsorption affinity of the fiber to the analyte. As shown in Table S1 (ESI†), the Co-NPC coated fiber had higher EFs (2811-4569, Table S1) to the OCPs than to the other aromatic compounds (≤ 976) and chlorinated straight-chain alkanes (<116). These phenomena can be explained by the structural characteristics of the relevant analytes. The low extraction efficiency of the fiber for 1-chlorohexane and 1-chlorooctane could be attributed to the lack of the π-π stacking interactions between the analytes and the Co-NPC coating. The large EF values for the OCPs can result from the presence of the delocalized π-system coming from their benzene ring and double bonds, which will form the π-π stacking interactions between the OCPs and the Co-NPC fiber coating. Meanwhile, for the same type of analytes, the compounds with higher log*P* values gave relatively higher EFs, suggesting that the hydrophobic interaction between the analytes and the Co-NPC coating plays a significant role in the SPME. For example, for the tested OCPs, with the gradual increase of the hydrophobicity (log*P*) of the compounds, the EF values were increased from *p,p'*-DDD (log*P*, 5.39) to *p,p'*-DDE (log*P*, 6.37). The higher EF values for the chlorobenzenes than those for the chlorophenols also suggest the influence of the hydrophobic interactions between the fiber coating and the analytes. In summary, the π-π stacking interaction and the hydrophobic interaction are the two main factors for the adsorption of the Co-NPC coating for the analytes, and the Co-NPC coating would be more suitable for the extraction of OCPs or other aromatic compounds.

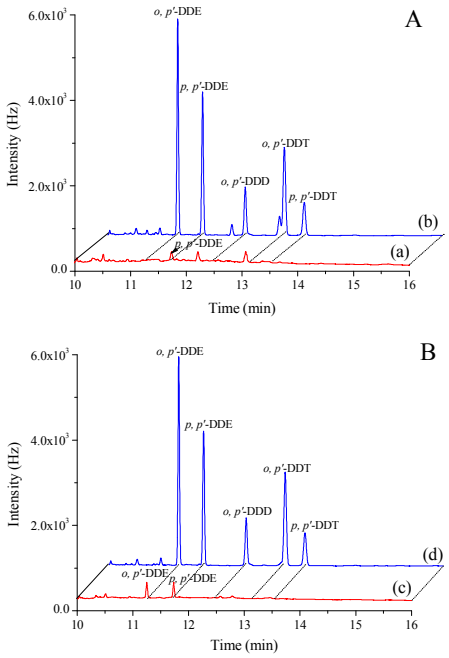

Fig. 7. Chromatograms of the extracts of OCPs from (A) cucumber and (B) celery cabbage samples. (a) Blank cucumber sample and (b) spiked cucumber sample at 20.0 ng g^{-1}. (c) Blank celery cabbage sample and (d) spiked celery cabbage sample at 20.0 ng g^{-1}.

Method evaluation and real sample analysis

The repeatability of the SPME-GC-μECD method (run-to-run RSD) was evaluated by performing five replicate analyses of the vegetable samples spiked with each of the analytes at 20.0 ng g^{-1} with the same Co-NPC coated fiber. The resulting RSDs varied between 4.9% and 9.6% (Table 1). To study the reproducibility of the preparation of the Co-NPC coated fibers (fiber-to-fiber RSD), five different fibers with equal dimensions prepared by the same procedures were used for the analysis of the same sample for evaluation. The RSDs were found in the range of 5.8- 11.0%. Fig. 6 shows that one single fiber could be used without a tangible change in the performance for about 100 extraction/desorption cycles. Calibration curves were obtained by analyzing eight concentration levels of the analytes spiked in OCPs-free cabbage, cucumber, and celery cabbage samples under the optimal extraction conditions. The following concentration levels were used: 0.2, 0.5, 1.0, 2.0, 5.0, 10.0, 20.0 and 50.0 ng g^{-1} for *o, p'*-DDE, *p, p'*-DDE and *o, p'*-DDT; 0.5, 1.0, 2.0, 5.0, 10.0, 20.0, 50.0 and 100 ng g^{-1} for *p, p'*-DDD and *p, p'*-DDT, respectively. The linearity existed over the concentration range from their corresponding limits of quantification (LOQs) to 50 ng g^{-1} for *o, p'*-DDE, *p, p'*-DDE and *o, p'*-DDT, and from their LOQs to 100 ng g^{-1} for *p, p'*-DDD and *p, p'*-DDT, respectively, with the determination coefficients ranging from 0.9923 to 0.9989. The limits of detection (LODs) and LOQs of the analytes were determined based on the signal-to-noise ratios of 3 and 10, respectively. Their LODs and LOQs were found to be between 0.09-0.45 and 0.30-1.50 ng g^{-1} in cabbage samples, 0.07-0.36 and 0.23-1.20 ng g^{-1} in cucumber samples, 0.09-0.34 and 0.30-1.13 ng g^{-1} in celery cabbage samples, respectively. The relevant data for the analytical characteristics of the established method are listed in Table 1.

To test the applicability of the established method, the method was applied to the analysis of different kinds of vegetables and the experimental results are shown in Table 2. The vegetable samples were purchased from a local market and treated according to the aforementioned procedures. The results indicated that no residues of the OCPs were detected out in the cabbage samples; only a low concentration of *p, p'*-DDE (2.76 ng g^{-1}) was found in cucumber samples; *o, p'*-DDE and *p, p'*-DDE were determined to be 2.69 ng g^{-1} and 4.08 ng g^{-1} in celery cabbage samples. To test the accuracy of the method, the recoveries of the five OCPs for the method were investigated by spiking the standard solution of the OCPs into the cabbage, cucumber and celery cabbage samples at 5.0 and 20.0 ng g^{-1}, respectively and then analyzing the spiked samples with the developed method. For each concentration level, five replicate experiments were performed. As shown in Table 2, the determined recoveries of the five OCPs were in the range from 87.9% to 98.2% with RSDs between 5.1% and 9.5% for cabbage sample, from 90.5% to 101.3% with RSDs between 5.6% and 8.9% for cucumber sample, and from 89.2% to 102.2% with RSDs under 10.4% for celery cabbage sample. These results demonstrate a good applicability of the established method for the analysis of trace-level OCPs in vegetables. The typical chromatograms of the cucumber and celery cabbage samples before and after being spiked with each of the OCPs at 20.0 ng g^{-1} are presented in Fig. 7.

A comparison of this method with the previously reported SPME methods[52-56] for the analysis of OCPs is summarized in Table S2 (see ESI†). The data in Table S2 shows that the method developed here has a comparable or even better performance in the respects of the LODs, linear range and RSDs.

Table 1 Analytical characteristics of the SPME-GC-μECD methods for the determination of OCPs in vegetable samples[a]

Samples	Pesticides	Linear range (ng g^{-1})	r^2	LODs (ng g^{-1})	LOQs (ng g^{-1})		Repeatability (*n*= 5, %)	Reproducibility (*n*= 5, %) fiber to fiber
Cabbage	*o, p'*-DDE	0.30- 50	0.9960	0.09	0.30	6.3		9.0
	p, p'-DDE	0.43- 50	0.9929	0.13	0.43	5.4		8.9
	p, p'-DDD	1.07- 100	0.9973	0.32	1.07	7.1		8.7
	o, p'-DDT	0.57- 50	0.9989	0.17	0.57	7.8		9.8
	p, p'-DDT	1.50- 100	0.9956	0.45	1.50	9.6		9.1
Cucumber	*o, p'*-DDE	0.23- 50	0.9979	0.07	0.23	4.9		6.1
	p, p'-DDE	0.37- 50	0.9950	0.11	0.37	6.4		9.5
	p, p'-DDD	0.90- 100	0.9949	0.27	0.90	5.5		7.4
	o, p'-DDT	0.47- 50	0.9988	0.14	0.47	7.3		11.0
	p, p'-DDT	1.20- 100	0.9923	0.36	1.20	8.2		9.8
Celery cabbage	*o, p'*-DDE	0.30- 50	0.9944	0.09	0.30	7.5		5.8
	p, p'-DDE	0.37- 50	0.9942	0.11	0.37	6.3		9.9
	p, p'-DDD	0.97- 100	0.9981	0.29	0.97	5.9		7.2
	o, p'-DDT	0.50- 50	0.9958	0.15	0.50	6.7		9.8
	p, p'-DDT	1.13- 100	0.9927	0.34	1.13	6.8		10.7

[a] Experimental conditions: Room temperature; extraction time, 30 min; stirring rate, 600 rpm; 15% KCl concentration; desorption temperature, 260 °C; desorption time, the whole run time.

Table 2 Analytical results for the determination of five OCPs in vegetables using the established SPME-GC-μECD method.

Pesticides	Spiked (ng g^{-1})	Cabbage (*n*= 5)			Cucumber (*n*= 5)			Celery cabbage (*n*= 5)		
		Found (ng g^{-1})	Recovery (%)	RSD (%)	Found (ng g^{-1})	Recovery (%)	RSD (%)	Found (ng g^{-1})	Recovery (%)	RSD (%)
	0	nd [a]			nd			2.69		
o, p'-DDE	5.0	4.91	98.2	7.2	4.53	90.6	8.7	7.56	97.4	7.6
	20.0	18.50	92.5	5.1	17.96	89.8	6.3	23.47	103.9	9.1
	0	nd			2.76			4.08		
p, p'-DDE	5.0	4.74	94.8	8.6	7.70	98.8	7.2	9.19	102.2	6.9
	20.0	18.86	94.3	5.7	23.02	101.3	8.9	23.80	98.6	5.4
	0	nd			nd			nd		
p, p'-DDD	5.0	4.55	91.0	8.0	4.86	97.2	8.6	4.89	97.8	9.2
	20.0	19.18	95.9	9.5	19.70	98.5	7.1	17.98	89.9	8.0
	0	nd			nd			nd		
o, p'-DDT	5.0	4.67	93.4	7.5	4.61	92.2	5.9	4.77	95.4	6.8
	20.0	19.62	98.1	5.6	18.92	94.6	5.6	19.94	99.7	6.5
	0	nd			nd			nd		
p, p'-DDT	5.0	4.49	89.8	9.4	4.57	91.4	7.4	4.46	89.2	10.4
	20.0	17.58	87.9	7.9	18.10	90.5	8.8	19.02	95.1	7.1

[a] nd: not detected.

Conclusions

In summary, a novel nanoporous carbon Co-NPC was successfully fabricated by one-step direct carbonization of ZIF-67 without using any other additional carbon precursors. The prepared Co-NPC was immobilized onto a stainless steel wire *via* a physical coating approach to get SPME fibers. The method by the SPME with the newly prepared fiber coupled with GC/μECD detection showed a satisfactory reproducibility, wide linear range and low LODs for the determination of OCPs. Moreover, good recoveries of the analytes were obtained when the method was used for the analysis of OCPs in vegetable samples, illustrating a feasibility of the method for the monitoring of the OCPs in vegetables. A comparison with the other counterparts for the SPME of OCPs regarding the LODs, linear range and RSDs shows that the current method has a comparable or even better performance.

Acknowledgments

The authors acknowledge the financial support of the National Natural Science Foundation of China (No. 31471643, 31571925), the Innovation Research Program of the Department of Education of Hebei for Hebei Provincial Universities (LJRC009), and the Scientific Research Program of Hebei Education Department (QN2014133).

Notes and references

1. C. L. Arthur and J. Pawliszyn, *Anal. Chem.*, 1990, **62**, 2145-2148.
2. F. Ghaemi, A. Amiri and R. Yunus, *TrAC Trends Anal. Chem.*, 2014, **59**, 133-143.
3. G. Ouyang, D. Vuckovic and J. Pawliszyn, *Chem. Rev.*, 2011, **111**, 2784-2814.
4. A. Mehdinia and M. O. Aziz-Zanjani, *TrAC Trends Anal. Chem.*, 2013, **42**, 205-215.
5. F. Zhu, Y. Liang, L. Xia, M. Rong, C. Su, R. Lai, R. Li and G. Ouyang, *J. Chromatogr. A*, 2012, **1247**, 42-48.
6. X. Wang, J. Liu, A. Liu, Q. Liu, X. Du and G. Jiang, *Anal. Chim. Acta*, 2012, **753**, 1-7.
7. S. L. Chong, D. Wang, J. D. Hayes, B. W. Wilhite and A. Malik, *Anal. Chem.*, 1997, **69**, 3889-3898.
8. M. Sun, J. Feng, Y. Bu, X. Wang, H. Duan and C. Luo, *Talanta*, 2015, **134**, 200-205.
9. L. Q. Yu and X. P. Yan, *Chem. Commun.*, 2013, **49**, 2142-2144.
10. S. Zhang, Z. Du and G. Li, *Anal. Chem.*, 2011, **83**, 7531-7541.
11. J. Wu, W. M. Mullett and J. Pawliszyn, *Anal. Chem.*, 2002, **74**, 4855-4859.
12. Q. Li, X. Wang and D. Yuan, *J. Chromatogr. A*, 2009, **1216**, 1305-1311.
13. A. Rahimi, P. Hashemi, A. Badiei, P. Arab and A. R. Ghiasvand, *Anal. Chim. Acta*, 2011, **695**, 58-62.
14. J. Zeng, C. Zhao, J. Chen, F. Subhan, L. Luo, J. Yu, B. Cui, W. Xing, X. Chen and Z. Yan, *J. Chromatogr. A*, 2014, **1365**, 29-34.
15. W. Zhang, Y. Sun, C. Wu, J. Xing and J. Li, *Anal. Chem.*, 2009, **81**, 2912-2920.
16. J. X. Wang, D. Q. Jiang, Z. Y. Gu and X. P. Yan, *J. Chromatogr. A*, 2006, **1137**, 8-14.
17. J. Feng, M. Sun, J. Li, X. Liu and S. Jiang, *Anal. Chim. Acta*, 2011, **701**, 174-180.
18. E. Ghasemi and M. Sillanpaa, *Talanta*, 2014, **130**, 322-327.
19. Y. Y. Wu, C. X. Yang and X. P. Yan, *J. Chromatogr. A*, 2014, **1334**, 1-8.
20. J. R. Li, J. Sculley and H. C. Zhou, *Chem. Rev.*, 2011, **112**, 869-932.
21. H. C. Zhou, J. R. Long and O. M. Yaghi, *Chem. Rev.*, 2012, **112**, 673-674.

22. S. K. Nune, P. K. Thallapally, A. Dohnalkova, C. Wang, J. Liu and G. J. Exarhos, *Chem. Commun.*, 2010, **46**, 4878-4880.
23. K. S. Park, Z. Ni, A. P. Côté, J. Y. Choi, R. Huang, F. J. Uribe-Romo, H. K. Chae, M. O'Keeffe and O. M. Yaghi, *Proc. Natl. Acad. Sci. USA*, 2006, **103**, 10186-10191.
24. X. Y. Cui, Z. Y. Gu, D. Q. Jiang, Y. Li, H. F. Wang and X. P. Yan, *Anal. Chem.*, 2009, **81**, 9771-9777.
25. N. Chang, Z. Y. Gu, H. F. Wang and X. P. Yan, *Anal. Chem.*, 2011, **83**, 7094-7101.
26. C. T. He, J. Y. Tian, S. Y. Liu, G. Ouyang, J. P. Zhang and X. M. Chen, *Chem. Sci.*, 2013, **4**, 351-356.
27. X. F. Chen, H. Zang, X. Wang, J. G. Cheng, R. S. Zhao, C. G. Cheng and X. Q. Lu, *Analyst*, 2012, **137**, 5411-5419.
28. L. Xie, S. Liu, Z. Han, R. Jiang, H. Liu, F. Zhu, F. Zeng, C. Su and G. Ouyang, *Anal. Chim. Acta*, 2015, **853**, 303-310.
29. H. B. Shang, C. X. Yang and X. P. Yan, *J. Chromatogr. A*, 2014, **1357**, 165-171.
30. J. Zheng, S. Li, Y. Wang, L. Li, C. Su, H. Liu, F. Zhu, R. Jiang and G. Ouyang, *Anal. Chim. Acta*, 2014, **829**, 22-27.
31. Y. A. Li, F. Yang, Z. C. Liu, Q. K. Liu and Y. B. Dong, *J. Mater. Chem. A*, 2014, **2**, 13868.
32. G. Wang, Y. Lei and H. Song, *Talanta*, 2015, **144**, 369-374.
33. Q. L. Li, X. Wang, X. F. Chen, M. L. Wang and R. S. Zhao, *J. Chromatogr. A*, 2015, **1415**, 11-19.
34. S. Liu, Y. Zhou, J. Zheng, J. Xu, R. Jiang, Y. Shen, J. Jiang, F. Zhu, C. Su and G. Ouyang, *Analyst*, 2015, **140**, 4384-4387.
35. D. D. Zu, L. Lu, X. Q. Liu, D. Y. Zhang and L. B. Sun, *J. Phys. Chem. C*, 2014, **118**, 19910-19917.
36. B. Liu, H. Shioyama, T. Akita and Q. Xu, *J. Am. Chem. Soc.*, 2008, **130**, 5390-5391.
37. H. L. Jiang, B. Liu, Y. Q. Lan, K. Kuratani, T. Akita, H. Shioyama, F. Zong and Q. Xu, *J. Am. Chem. Soc.*, 2011, **133**, 11854-11857.
38. A. Aijaz, N. Fujiwara and Q. Xu, *J. Am. Chem. Soc.*, 2014, **136**, 6790-6793.
39. W. Chaikittisilp, K. Ariga and Y. Yamauchi, *J. Mater. Chem. A*, 2013, **1**, 14-19.
40. M. Hu, J. Reboul, S. Furukawa, N. L. Torad, Q. Ji, P. Srinivasu, K. Ariga, S. Kitagawa and Y. Yamauchi, *J. Am. Chem. Soc.*, 2012, **134**, 2864-2867.
41. A. Almasoudi and R. Mokaya, *J. Mater. Chem.*, 2012, **22**, 146-152.
42. S. J. Yang, T. Kim, J. H. Im, Y. S. Kim, K. Lee, H. Jung and C. R. Park, *Chem. Mater.*, 2012, **24**, 464-470.
43. R. Banerjee, A. Phan, B. Wang, C. Knobler, H. Furukawa, M. O'Keeffe and O. Yaghi, *Science*, 2008, **319**, 939-943.
44. X. Liu, C. Wang, Q. Wu and Z. Wang, *Anal. Chim. Acta*, 2015, **870**, 67-74.
45. L. Zhao, H. Hou, Y. Shangguan, B. Cheng, Y. Xu, R. Zhao, Y. Zhang, X. Hua, X. Huo and X. Zhao, *Ecotoxicol. Environ. Saf.*, 2014, **108**, 120-128.
46. Y. Lu, W. Zhan, Y. He, Y. Wang, X. Kong, Q. Kuang, Z. Xie and L. Zheng, *ACS Appl. Mater. Interfaces*, 2014, **6**, 4186-4195.
47. J. Shao, Z. Wan, H. Liu, H. Zheng, T. Gao, M. Shen, Q. Qu and H. Zheng, *J. Mater. Chem. A*, 2014, **2**, 12194-12200.
48. N. L. Torad, M. Hu, S. Ishihara, H. Sukegawa, A. A. Belik, M. Imura, K. Ariga, Y. Sakka and Y. Yamauchi, *Small*, 2014, **10**, 2096-2107.
49. J. Ai and A. Chem., *Anal. Chem.*, 1997, **69**, 1230-1236.
50. M. T. Jafari, M. Saraji and H. Sherafatmand, *Anal. Chim. Acta*, 2014, **814**, 69-78.
51. H. Asadollahzadeh, E. Noroozian and S. Maghsoudi, *Anal. Chim. Acta*, 2010, **669**, 32-38.
52. D. A. Lambropoulou, I. K. Konstantinou and T. A. Albanis, *Anal. Chim. Acta*, 2006, **573-574**, 223-230.
53. J. A. Cai, F. Zhu, W. Ruan, L. Liu, R. Lai, F. Zeng and G. Ouyang, *Microchem. J.*, 2013, **110**, 280-284.
54. J. Zeng, J. Chen, Z. Lin, W. Chen, X. Chen and X. Wang, *Anal. Chim. Acta*, 2008, **619**, 59-66.
55. P. N. Carvalho, P. N. Rodrigues, F. Alves, R. Evangelista, M. C. Basto and M. T. Vasconcelos, *Talanta*, 2008, **76**, 1124-1129.
56. M. Fernandez-Alvarez, M. Llompart, J. P. Lamas, M. Lores, C. Garcia-Jares, R. Cela and T. Dagnac, *J. Chromatogr. A*, 2008, **1188**, 154-163.